Light Sources and Free Electron Lasers

Steve Lidia

This material is based upon work supported by the U.S. Department of Energy Office of Science under Cooperative Agreement DE-SC0000661, the State of Michigan and Michigan State University. Michigan State University designs and establishes FRIB as a DOE Office of Science National User Facility in support of the mission of the Office of Nuclear Physics.

Outline

- Introduction
- Insertion device radiation
  - Time dilation effects
  - Bending magnet, undulators, wigglers
- Synchrotron light sources
  - Energy trade-offs
  - Experiments
  - Achieving higher brightness
- Free electron lasers (FELs)
  - Gain and spectrum
  - Fully coherent x-rays

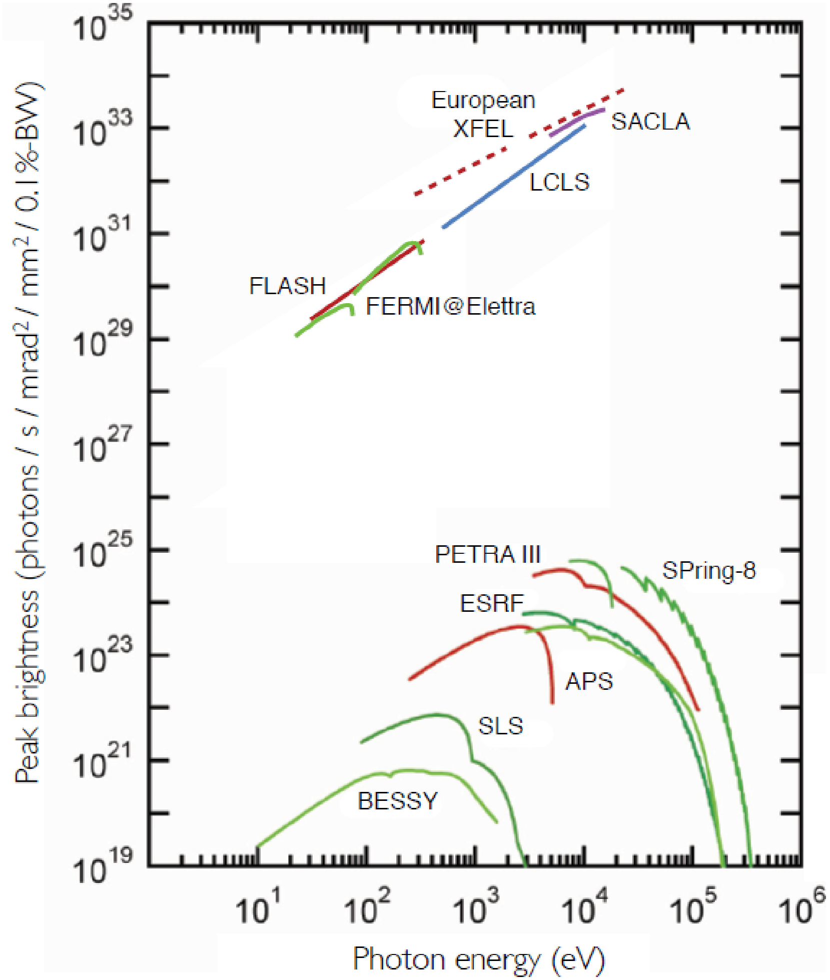

Laser Technologies Span THz to UV

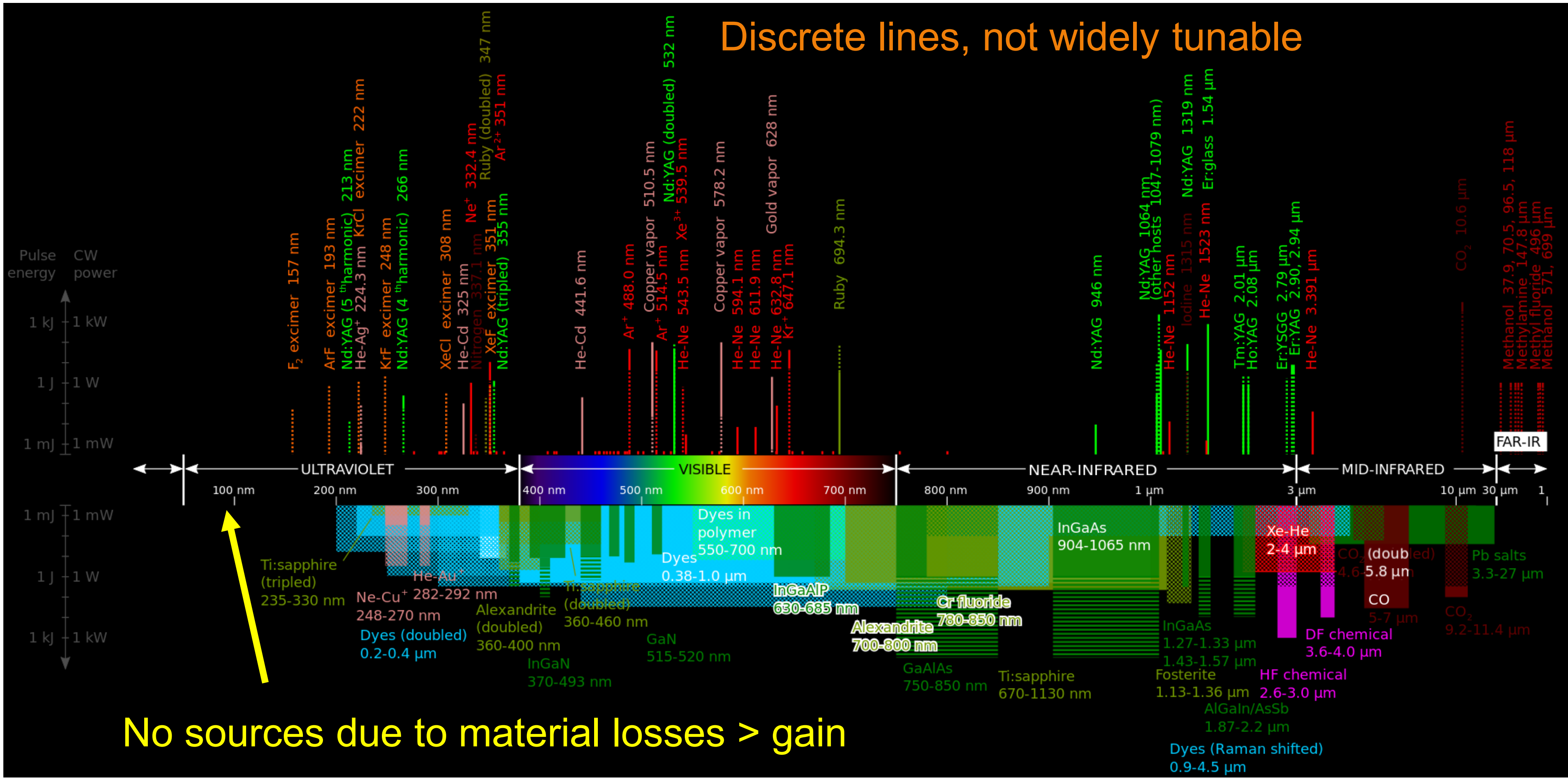

Laboratory Radiation Source Development

- Tunable radiation sources based on electron beams
  - Developed over decades from ‘tubes’
- Fill gaps in laser spectra and optics
- Tailored for experiments and applications.

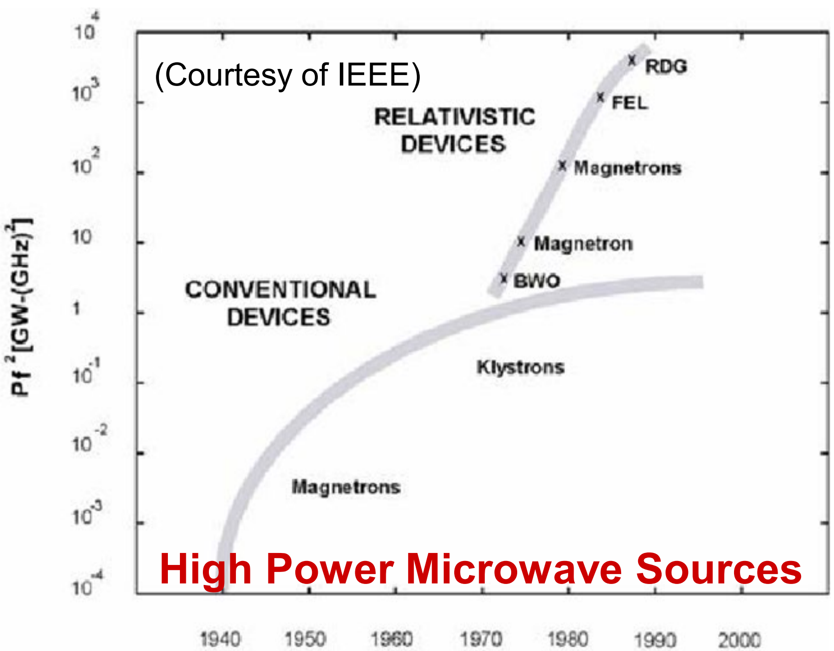

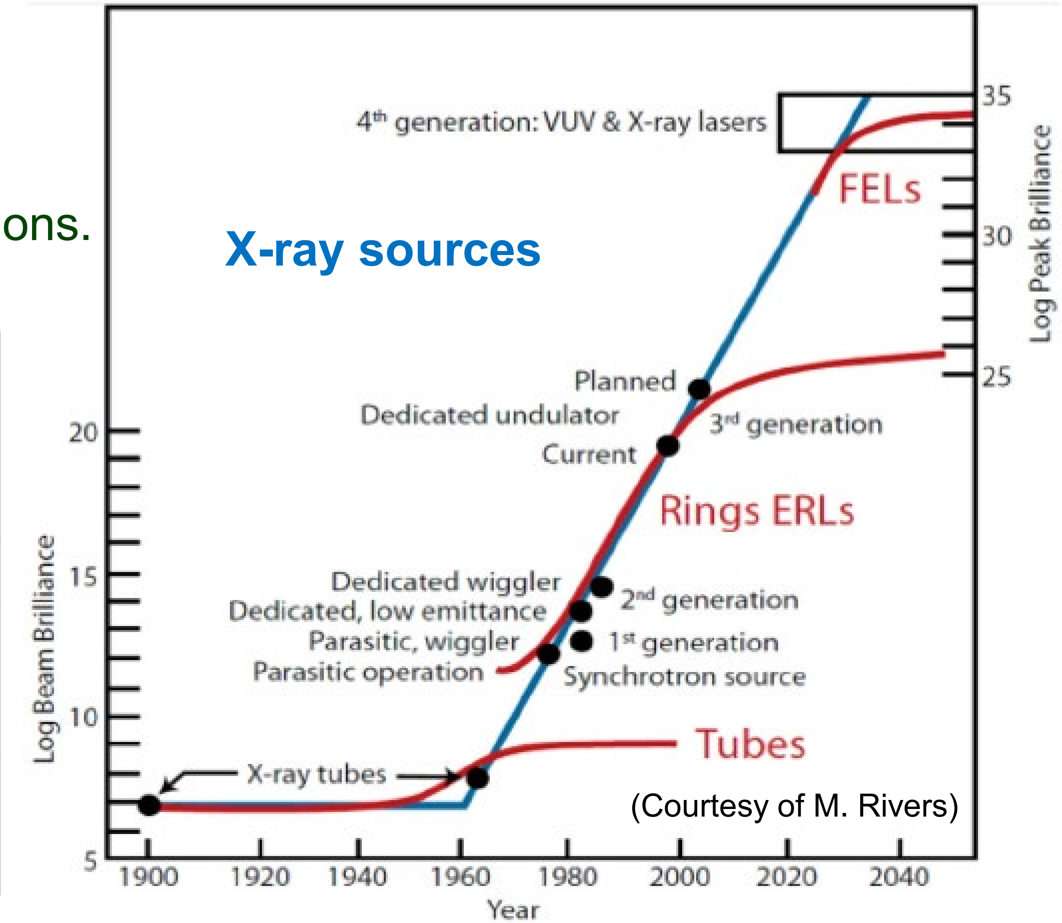

Radiation from Charged Particles

- The treatment of the radiation field emitted from charged particles follows classically from Larmor and Lienard-Wiechert.

$$P_{Larmor} = \frac{2}{3}\frac{e^2}{4\pi\varepsilon_0 c^3}a^2 \qquad \frac{dP}{d\Omega} = \frac{1}{4\pi}\frac{e^2}{4\pi\varepsilon_0 c^3}a^2\sin^2\theta$$

‘a’ is apparent acceleration

$$\frac{dP(t')}{d\Omega} = \frac{1}{4\pi}\frac{e^2a^2}{4\pi\varepsilon_0 c^3}\frac{\sin^2\theta}{(1-\beta\cos\theta)^5}$$

Acceleration ∥ velocity

$$\frac{dP(t')}{d\Omega} = \frac{1}{4\pi}\frac{e^2a^2}{4\pi\varepsilon_0 c^3}\frac{(1-\beta\cos\theta)^2-(1-\beta^2)\sin^2\theta\cos^2\theta}{(1-\beta\cos\theta)^5}$$

Acceleration ⊥ velocity

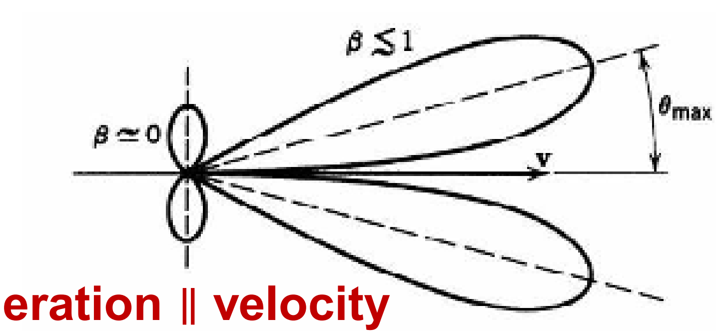

Acceleration ∥ velocity

J.D. Jackson (1998)

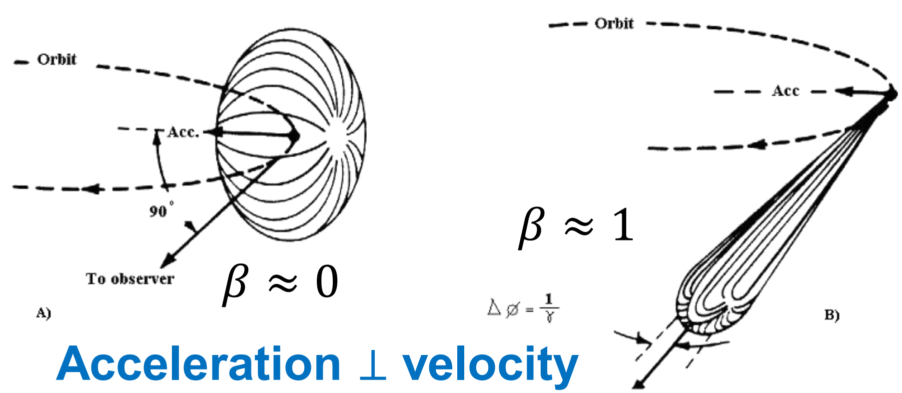

Acceleration ⊥ velocity

Relativistic effects in time dilation

- Emitter time vs Observer time

$$t_{obs} = t'_{emit} + R(t')/c$$

- Scale factor $\Delta t \approx \kappa(t')\Delta t'$

$$\kappa(t') = \frac{dt}{dt'} = 1 - \boldsymbol{n}(t')\cdot\boldsymbol{\beta}(t') = 1 - \beta\cos\theta$$

$$1-\beta \approx \frac{1}{2\gamma^2} \ll 1 \Rightarrow \kappa \approx \frac{1}{2}\left(\frac{1}{\gamma^2}+\theta^2\right)\ ;\ \theta \ll 1$$

$$\boxed{\Delta t \approx \frac{\Delta t'}{\gamma^2};\ \theta \leq \gamma^{-1}}$$

$$\boxed{\frac{d^2x}{dt^2} \sim \frac{\Delta x}{(\Delta t)^2} \sim \gamma^4\frac{c^2}{\rho}}$$

Bending Magnet

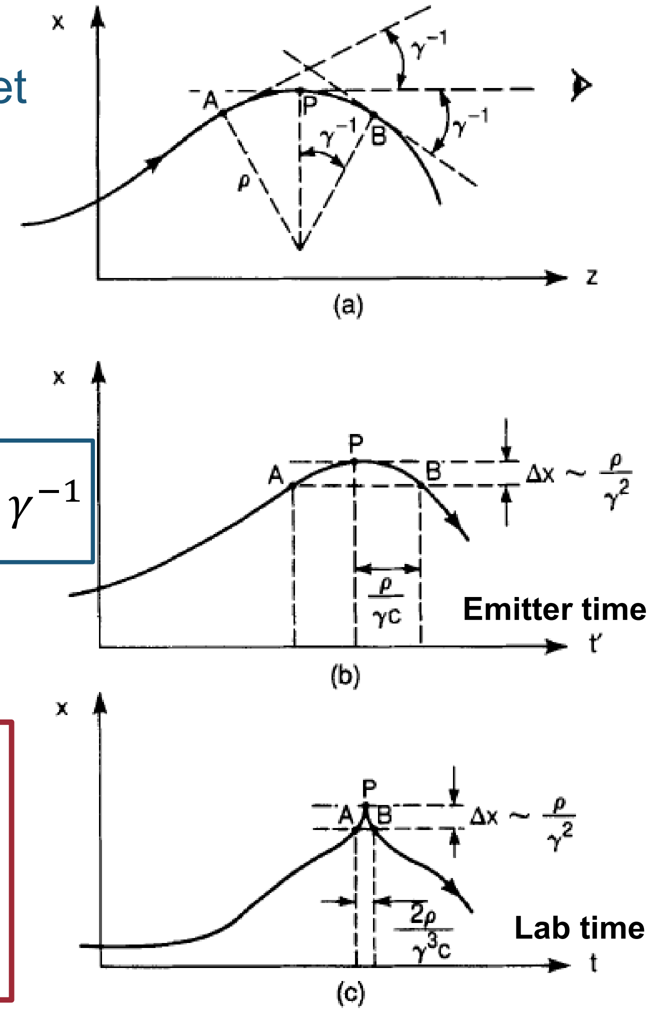

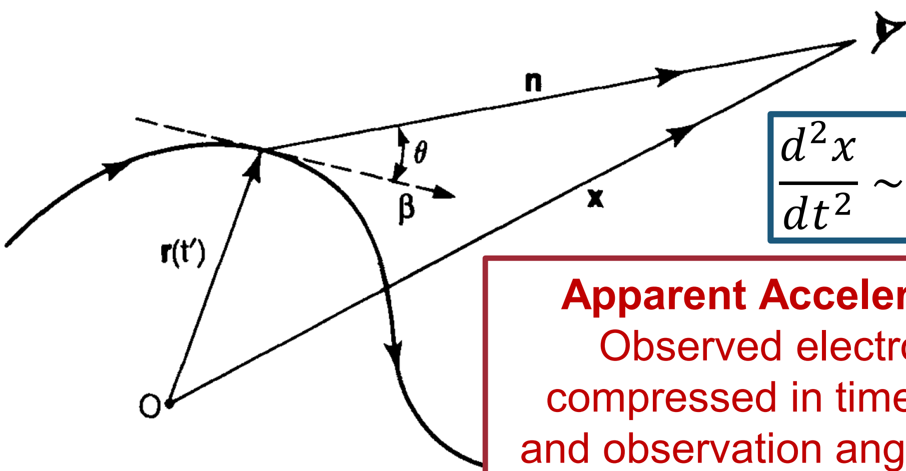

Figure 2.1 The electron trajector

Apparent Acceleration Effects
Observed electron motion is compressed in time when velocity and observation angle are aligned to within γ^{-1}

Undulators and Wiggler Motion

- We increase the number of emitters by creating specialized magnet devices, undulators and wigglers, with multiple poles.

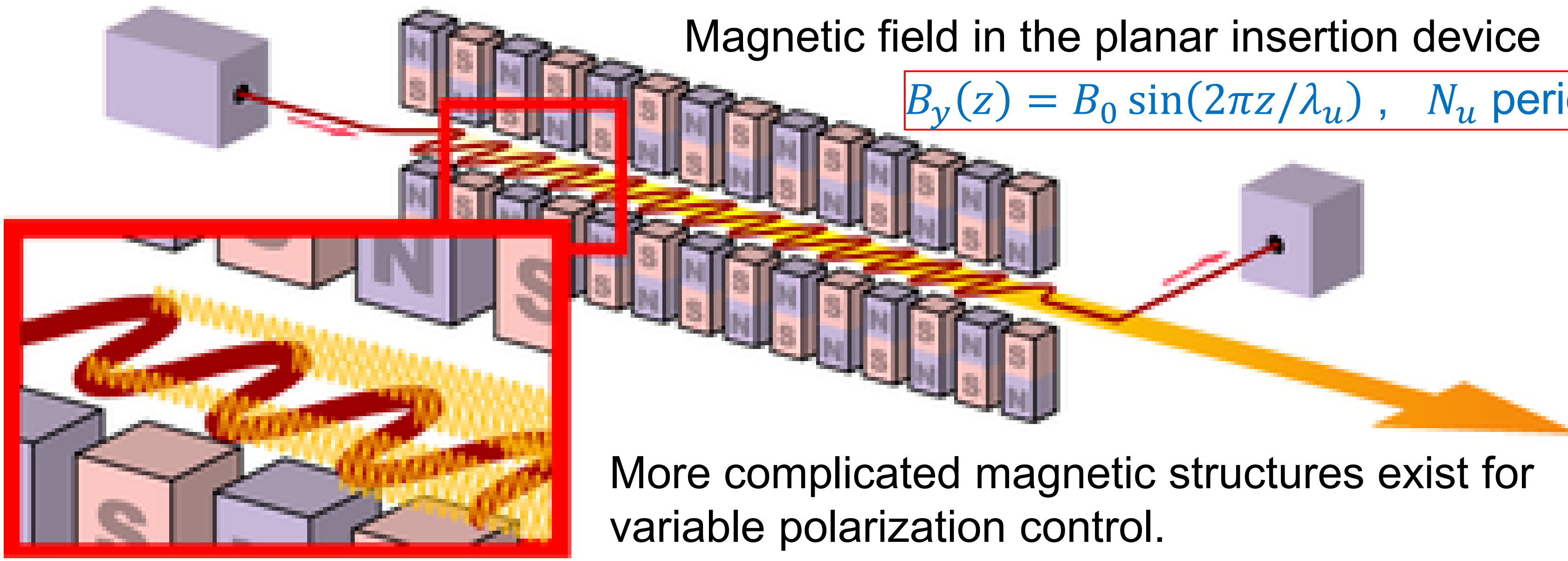

Magnetic field in the planar insertion device

$B_y(z) = B_0 \sin(2\pi z/\lambda_u)$, N_u periods

More complicated magnetic structures exist for variable polarization control.

Pure permament magnet (PPM) scaling of peak field with full gap, *g*, between jaws

$$B_0[T] = 3.44 \exp\left[-\frac{g}{\lambda_u}\left(5.08 - 1.54\frac{g}{\lambda_u}\right)\right]; NdFeB$$

$$B_0[T] = 3.33 \exp\left[-\frac{g}{\lambda_u}\left(5.47 - 1.8\frac{g}{\lambda_u}\right)\right]; SmCo$$

Insertion Devices

LCLS
PM
Undulator
Prototype

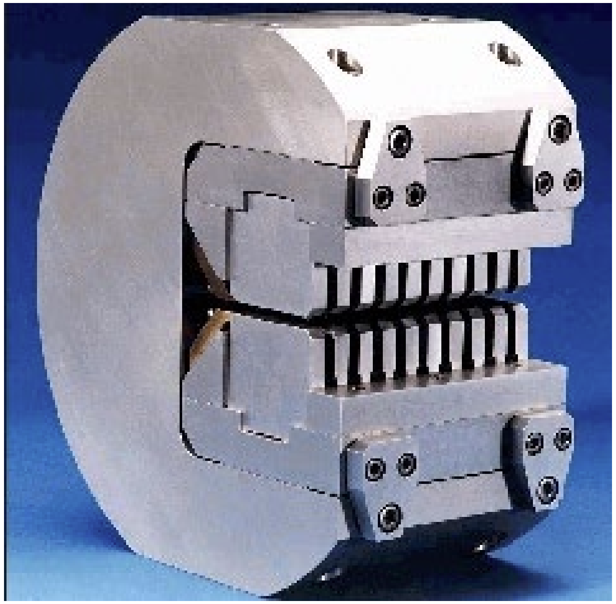

SRC University of Wisconsin Madison
EM Wiggler

SLAC
PM Undulator

DESY
PM Undulator

Lorentz Force Governs Motion

$$\vec{F} = q\left(\vec{E} + \vec{v} \times \vec{B}\right) \Longrightarrow \frac{d\vec{p}}{dt} = q\left(\vec{v} \times \vec{B}\right)$$

$$\frac{d\vec{p}}{dt} = \frac{d}{dt}\left(\gamma\vec{\beta}mc\right) = \gamma mc\frac{d\vec{\beta}}{dt}$$

$$q\left(\vec{v} \times \vec{B}\right) = -ec\left(\vec{\beta} \times \vec{B}\right)$$

$$\frac{d\vec{\beta}}{dt} = \frac{-e}{\gamma m}\left(\vec{\beta} \times \vec{B}\right)$$

$$\frac{d\beta_x}{dt} = \frac{-e}{\gamma m}\left(\beta_y B_z - \beta_z B_y\right) \Longrightarrow \frac{d\beta_x}{dt} = \frac{e}{\gamma m}\beta_z B_y$$

0th order – constant β_z
1st order – oscillatory β_x
2nd order – oscillatory β_z

$\gamma \gg 1$

$\beta_z \sim 1 \gg \beta_x$

$$\frac{d\beta_x}{dt} = \frac{e}{\gamma m}\beta_z B_y = \frac{e\beta_z B_o}{\gamma m}\sin(2\pi z/\lambda_u)$$

$$\frac{d}{dt} \Longrightarrow \beta_z c\frac{d}{dz}$$

$$\boxed{\frac{d\beta_x}{dz} = \frac{eB_o}{\gamma mc}\sin(2\pi z/\lambda_u)}$$

Equations of Motion from Lorentz Force

- Electron transverse velocity

$$\beta_x = \frac{K}{\gamma}\cos(2\pi z/\lambda_u) \quad \text{where} \quad K = \frac{eB_0\lambda_u}{2\pi mc} = 0.934\lambda_u[cm]B_0[T]$$

- The maximum slope in the trajectory is $\delta = K/\gamma$
- We differentiate between 'undulator' ($K \lesssim 1$) and 'wiggler' motion (K>1)
- The longitudinal velocity, $c\beta_z$, is found

$$\beta_z = \sqrt{1 - \frac{1}{\gamma^2} - \beta_x^2} \approx 1 - \frac{1 + \frac{K^2}{2}}{2\gamma^2} - \frac{K^2}{4\gamma^2}\cos(4\pi z/\lambda_u)$$

- And displacement (with $\omega_u = 2\pi c/\lambda_u$)

$$\frac{1}{c}\vec{r}(t') = \left[\frac{K}{\gamma\omega_u}, 0, \underbrace{\left(1 - \frac{1 + \frac{K^2}{2}}{2\gamma^2}\right)}_{\text{Longitudinal 'slippage'}} t' - \frac{K^2}{8\gamma^2\omega_u}\sin(2\omega_u t')\right]$$

'Figure-8' motion

B.M. Kincaid, J. Appl. Phys., 48 (1977), 2684-2691.
K.J. Kim, AIP Conf. Proc. 184, 565 (1989).

Beam-frame and Lab-frame Motion

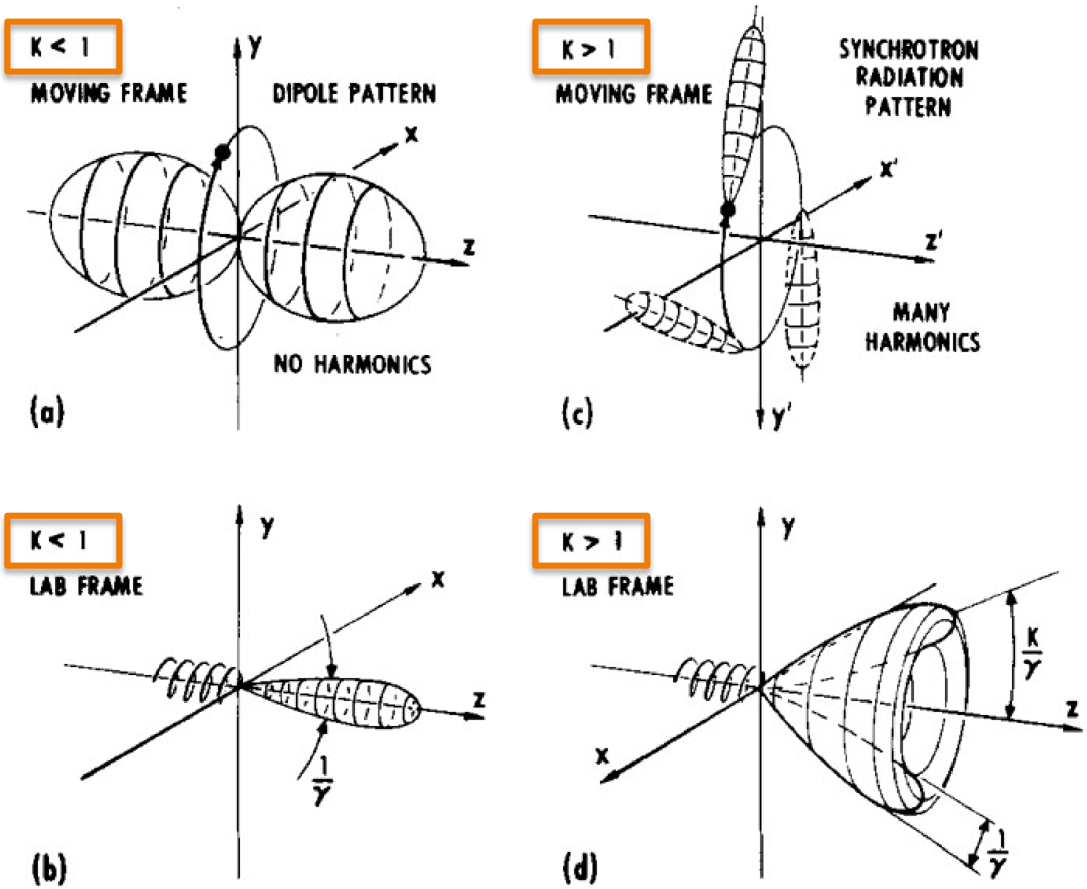

FIG. 2. Schematic representative of radiation produced in strong- and weak-field cases viewed both in the lab and in the moving frame.

B.M. Kincaid, J. Appl. Phys., **48** (1977), 2684-2691.

Equations of Motion - Longitudinal

- The unit observation vector, ***n***, is approximated by (with $\theta, \phi, \psi \sim \frac{1}{\gamma} \ll 1$)
  $\boldsymbol{n} \approx (\varphi, \psi, 1-\theta^2/2)$, and $\theta^2 = \phi^2 + \psi^2$
- The observer time (t) is then

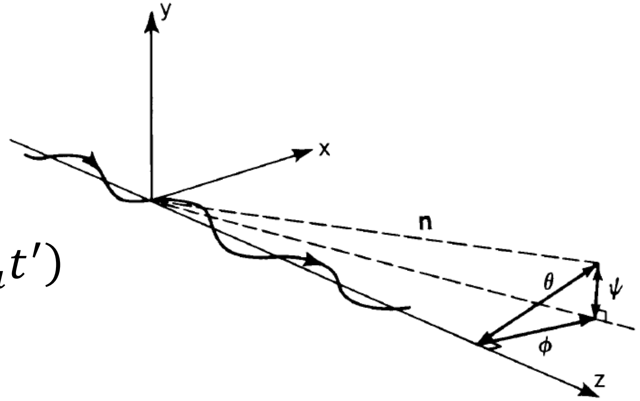

Figure 4.2 Coordinate system for the undulator radiation.

$$t = t' \frac{1 + \frac{K^2}{2} + \gamma^2\theta^2}{2\gamma^2} + \frac{K^2}{8\omega_u\gamma^2}\sin(2\omega_u t') - \frac{K\phi}{\omega_u\gamma}\sin(\omega_u t')$$

- Multiply by $\omega_1(\theta) = \frac{2\gamma^2}{1+\frac{K^2}{2}+\gamma^2\theta^2}\omega_u$
- To obtain $\omega_1(\theta)t = \omega_u t' + \frac{K^2}{4\left(1+\frac{K^2}{2}+\gamma^2\theta^2\right)}\sin(2\omega_u t') - \frac{2\gamma K\phi}{1+\frac{K^2}{2}+\gamma^2\theta^2}\sin(\omega_u t')$
- The apparent motion is **periodic** in time with period $2\pi/\omega_1(\theta)$ but **not sinusoidal**.
- The period is shorter than the period in the electron emitter time by a large factor.
- Undulator radiation exhibits sharp spectral peaks at _odd_ multiples of $\omega_1(\theta)$ _on-axis_.

K.J. Kim, AIP Conf. Proc. 184, 565 (1989).

Intensity and Spectral Characteristics

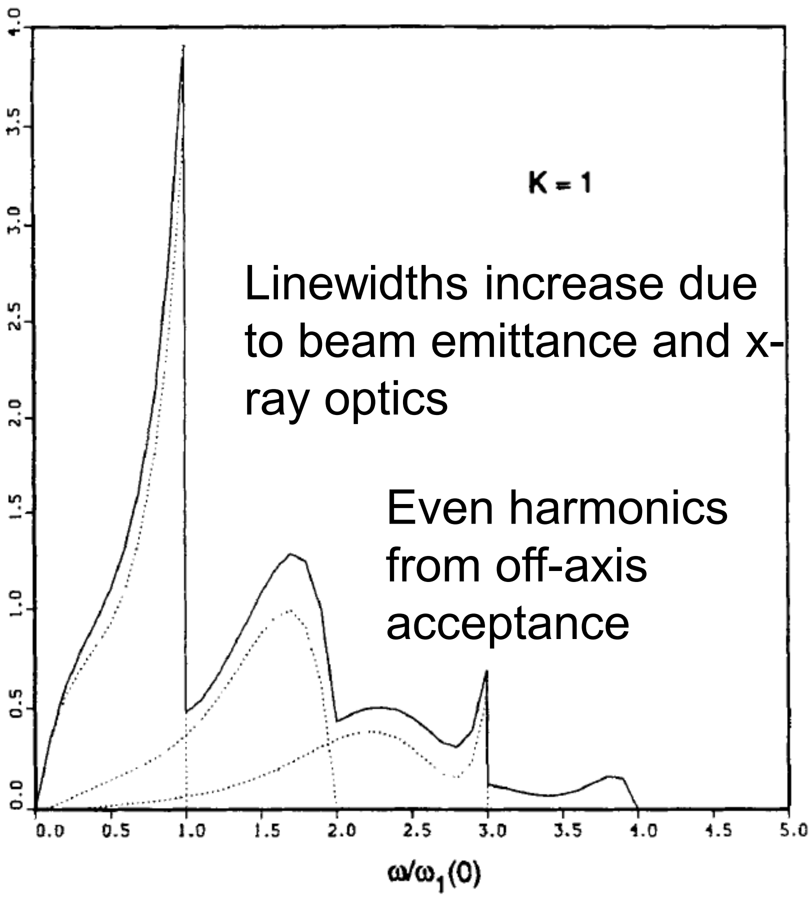

Linewidths increase due to beam emittance and x-ray optics

Even harmonics from off-axis acceptance

Figure 4.9 The angle-integrated undulator spectrum for K = 1. The dotted lines are individual harmonics and the solid line is their sum, including up to the 4th harmonic.

The radiation from an undulator has bandwidth **$\Delta\omega/\omega$ = 1/2N_u** (where N_u is the number of periods in the undulator), and is emitted in a cone with opening angle $1/\gamma$.

The on-axis intensity in the 1st harmonic is

$$\frac{dI}{d\Omega d\omega}(\theta = 0) = N_u^2 \frac{e^2}{c} \gamma^2 \frac{K^2/2}{(1+K^2/2)^2} [JJ]^2$$

Where $[JJ] = J_1\left(\frac{K^2/4}{(1+K^2/2)^2}\right) - J_0\left(\frac{K^2/4}{(1+K^2/2)^2}\right)$

K.J. Kim, AIP Conf. Proc. 184, 565 (1989).

Brightness and Coherence [1]
Electron beam size effects

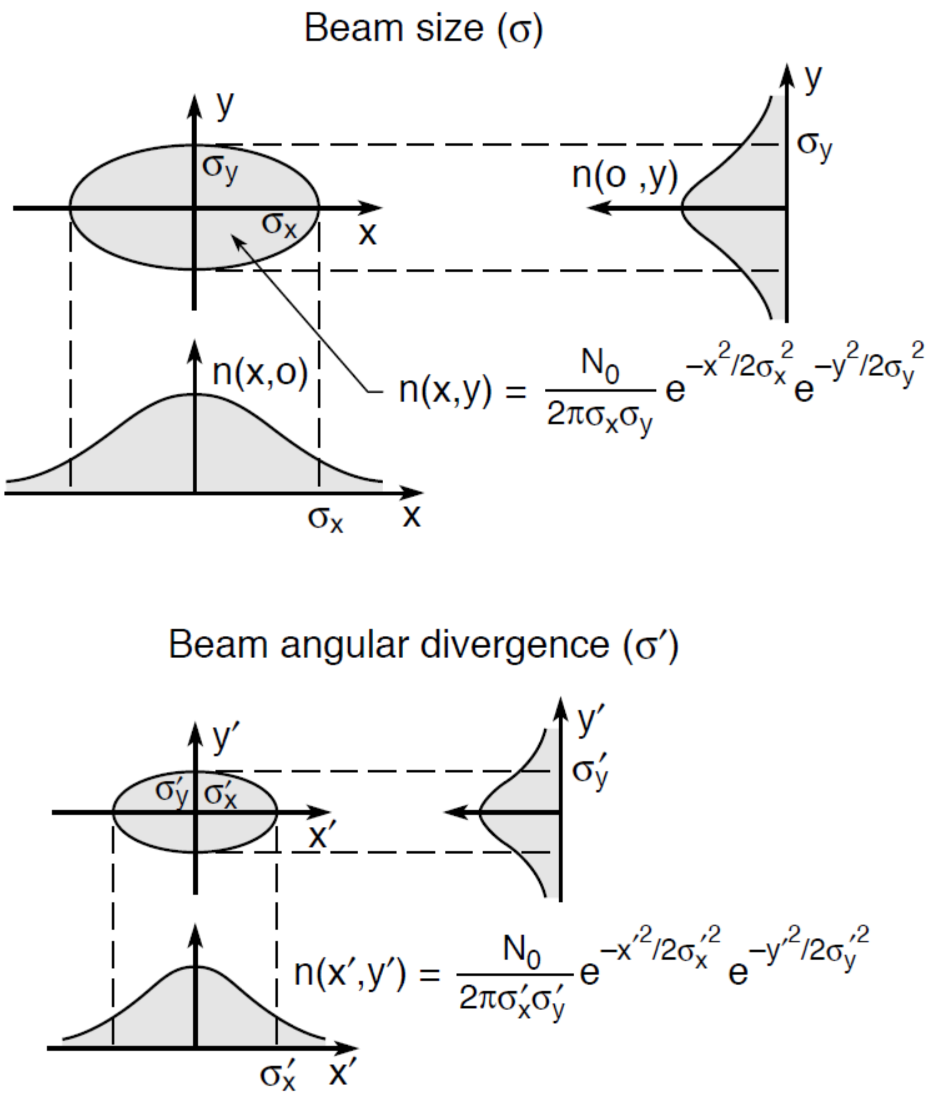

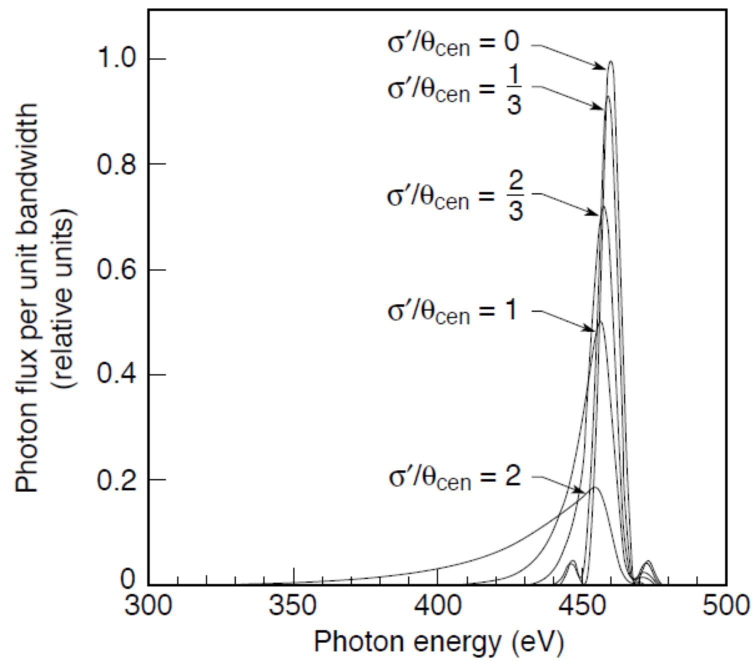

Preserving the spectral line shape of undulator radiation requires

$$\sigma'^2 \ll \theta_{\mathrm{cen}}^2 \qquad (5.55\mathrm{b})$$

Define effective, or total central cone half-angles

$$\theta_{Tx} = \sqrt{\theta_{\mathrm{cen}}^2 + \sigma_x'^2} \quad \text{and} \quad \theta_{Ty} = \sqrt{\theta_{\mathrm{cen}}^2 + \sigma_y'^2} \qquad (5.56)$$

Courtesy D. Attwood

Bending Magnet, Wiggler, Undulator

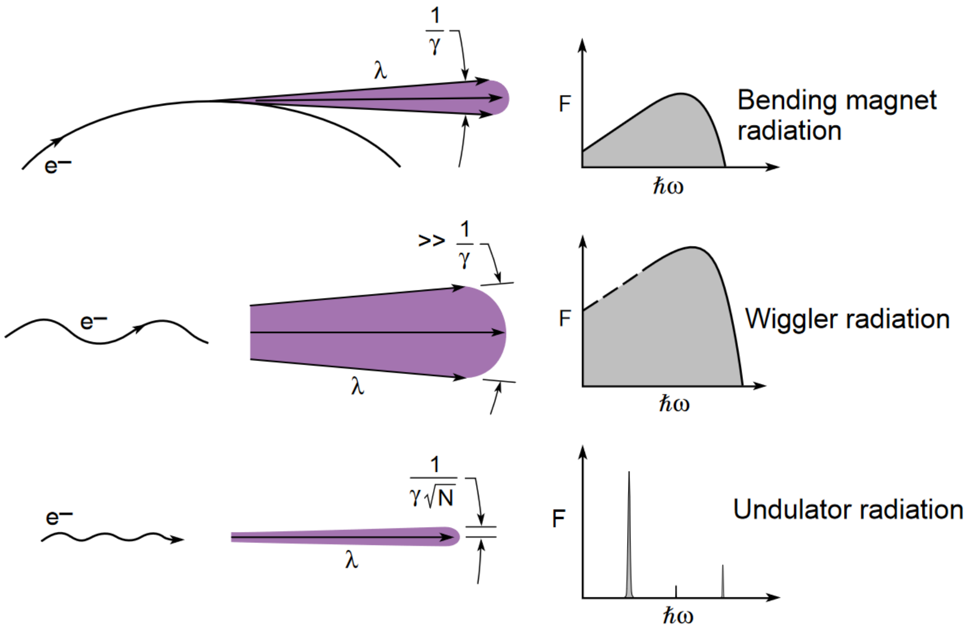

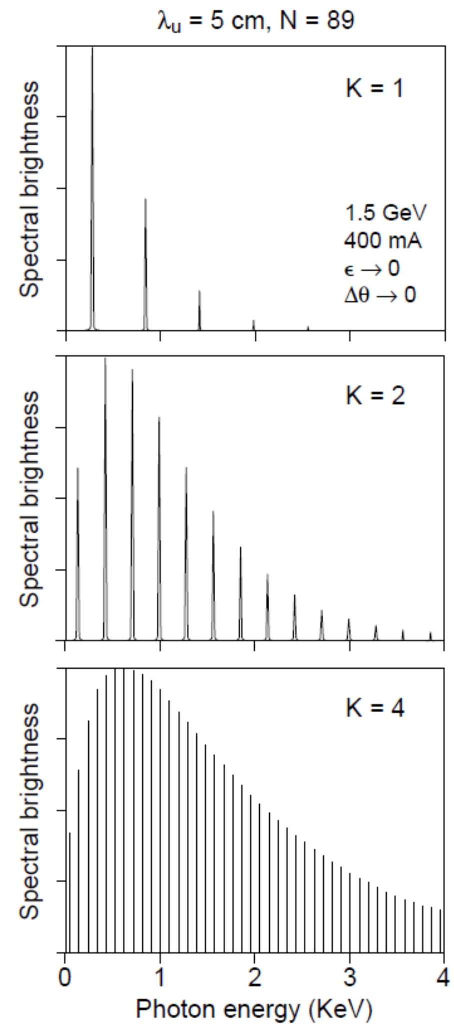

(Courtesy of K.-J. Kim)

Undulator radiation ($K \lesssim 1$)

- Narrow spectral lines
- High spectral brightness
- Partial coherence

$$\lambda = \frac{\lambda_u}{2\gamma^2}\left(1 + \frac{K^2}{2} + \gamma^2\theta^2\right)$$

$$K = \frac{eB_o\lambda_u}{2\pi mc}$$

Wiggler radiation ($K >> 1$)

- Higher photon energies
- Spectral continuum
- Higher photon flux (2N)

$$\hbar\omega_c = \frac{3}{2}\frac{\hbar\gamma^2 eB_o}{m}$$

$$n_c = \frac{3K}{4}\left(1 + \frac{K^2}{2}\right)$$

Brightness

$$\boxed{B = \frac{\Delta P}{\Delta A \cdot \Delta\Omega}}$$

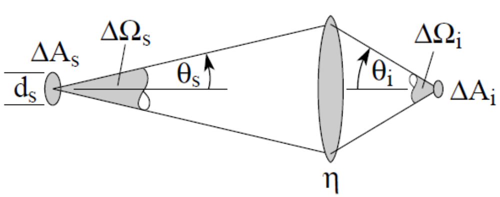

Spectral Brightness

$$\boxed{B_{\Delta\omega/\omega} = \frac{\Delta P}{\Delta A \cdot \Delta\Omega \cdot \Delta\omega/\omega}}$$

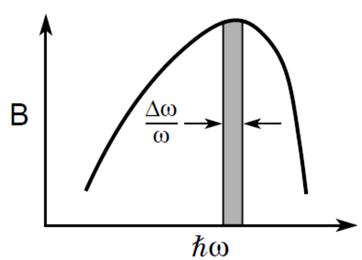

Perfect optical system:
$\Delta A_s \cdot \Delta\Omega_s = \Delta A_i \cdot \Delta\Omega_i$; $\eta = 100\%$

Conservation of photon phase space

Optical Beamline

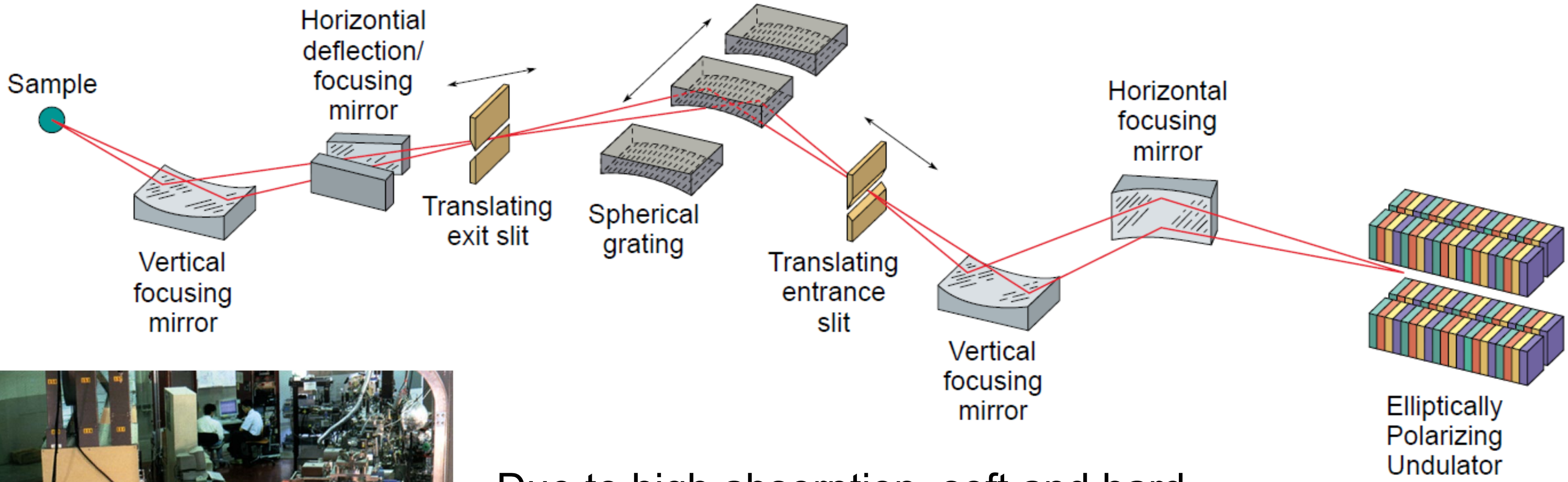

Due to high absorption, soft and hard x-ray optics are typically made from multi-layer Bragg reflectors, bent for focusing - “Kirkpatrick-Baez” geometry

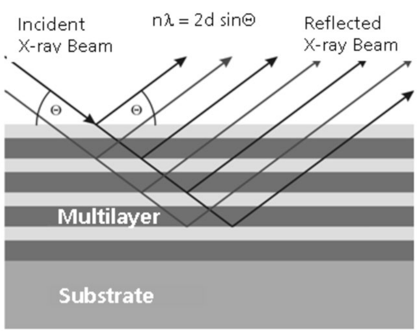

Some EUV focusing optics are transmissive, based on high-order Fresnel lenses.

See https://www.cxro.lbl.gov/

Brightness and Coherence [2]
Transverse Coherence

- Diffraction limited radiation fields can be described by modes (cf. Yariv, Siegman, Loudon, etc.)
- Coherent modes have propagation characteristics:
  - Wavelength λ, Rayleigh length Z_R, waist σ_r
  - Divergence $\sigma_{r'}$ $\qquad Z_R = \sigma_r / \sigma_{r'}$
  - Lowest order mode is Gaussian
    - » $\sigma_r(z) = \sqrt{\frac{\lambda}{4\pi}\left(Z_R + \frac{z^2}{Z_R}\right)}$ $\quad \sigma_{r'}(z) = \sigma_{r'}$ $\qquad$ At z=0: $\quad \sigma_r \sigma_{r'} = \frac{\lambda}{4\pi} = \varepsilon_{r,min}$

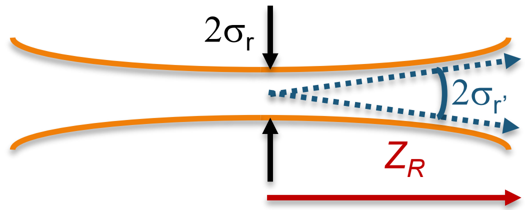

Photon beam emittance

- Overlap with electron beam $(\sigma_x, \sigma_{x'})$ produces the resultant radiation pattern
  - $\Sigma_x = \sqrt{\sigma_x{}^2 + \sigma_r{}^2}$ $\qquad \Sigma_{x'} = \sqrt{\sigma_{x'}{}^2 + \sigma_{r'}{}^2}$
  - If the electron beam moments are negligible with respect to the radiation mode
    - » $\Sigma_x \Sigma_{x'} \approx \sigma_r \sigma_{r'} = \frac{\lambda}{4\pi}$ $\qquad$ 'diffraction-limited radiation', transversely coherent
  - If the electron beam moments dominate the radiation mode
    - » $\Sigma_x \Sigma_{x'} \gg \frac{\lambda}{4\pi}$ $\qquad$ 'incoherent radiation'
  - Intermediate case is 'partially coherent' radiation
    - » No. of coherent modes is represented by
    - » $M_T = \frac{\Sigma_x \Sigma_{x'}}{\lambda/4\pi} \approx \frac{\varepsilon_x}{\varepsilon_r}$

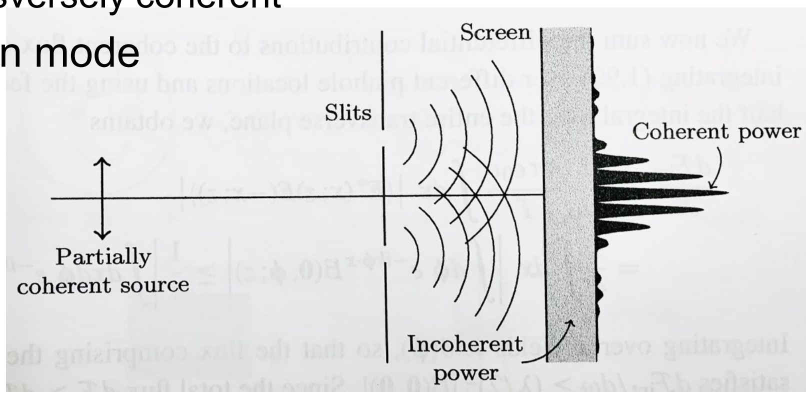

Brightness and Coherence [3]
Longitudinal Coherence

- Assume each electron in the bunch emits photons independently and randomly
  - $E(t) = \sum_{j=1}^{N_e} E_0(t-t_j) = e_0 \sum_{j=1}^{N_e} exp\left[-\frac{(t-t_j)^2}{4{\sigma_\tau}^2} - i\omega_r(t-t_j)\right]$ total radiation electric field
  - $E(\omega) = \frac{e_0\sqrt{\pi}}{\sigma_\omega}\sum_{j=1}^{N_e} exp\left[-\frac{(\omega-\omega_r)^2}{4{\sigma_\omega}^2} + i\omega_r t_j\right]$ frequency description (Fourier transform), with $\sigma_\omega = 1/\sigma_\tau$
- Define coherence time, t_{coh}, of optical field $E_0(t) = e_0 exp\left[-\frac{(t-t_j)^2}{4{\sigma_\tau}^2} - i\omega_r(t-t_j)\right]$ via
  - $t_{coh} = \int d\tau |C(\tau)|^2 = 2\sqrt{\pi}\sigma_\tau$ where the 1st order correlation function is
  - $C(\tau) \equiv \frac{\langle \int dt\, E(t)E^*(t+\tau)\rangle}{\langle \int dt\, E(t)E^*(t)\rangle}$ where ⟨ ⟩ indicates the ensemble average of sources
- Consider an observation time T_{obs}
- The no. of *longitudinal modes, M_L*, is $M_L \approx \frac{T_{obs}}{t_{coh}} \approx \frac{T_{obs}}{4\sigma_\tau}$

$${\sigma_{N_{ph}}}^2 = \frac{\langle N_{ph}\rangle^2}{M_L}$$

Fluctuation in photon number in observation period

- Considering quantum statistics (degeneracy) ${\sigma_{N_{ph}}}^2 = \frac{\langle N_{ph}\rangle^2}{M} + \langle N_{ph}\rangle \quad M = M_L {M_T}^2$
- Back to the electrons . . . $\langle |E(\omega)|^2\rangle = |E_{\omega 0}|^2 \left\langle \left|\sum_{j=1}^{N_e} exp[-i\omega_r t_j]\right|^2 \right\rangle = |E_{\omega 0}|^2 \left\{ N_e + \left\langle \sum_{j\neq k}^{N_e} exp[-i\omega_r(t_j - t_k)]\right\rangle \right\}$
- Electrons longitudinal distribution $f(t), \tilde{f}(\omega) \rightarrow \left\langle \sum_{j\neq k}^{N_e} exp[i\omega_r(t_j-t_k)]\right\rangle = N_e(N_e-1)\left|\tilde{f}(\omega)\right|^2$
- $\langle |E(\omega)|^2\rangle = N_e |E_{\omega 0}|^2 \left[1 + (N_e - 1)\left|\tilde{f}(\omega)\right|^2\right]$

Coherent enhancement if electron distribution has structure (microbunching) at frequency ω

Electron Rings As Light Sources

	Elettra	ALBA	DLS	ESRF	APS	SPring-8
Energy	2 GeV	3 GeV	3 GeV	6 GeV	7 GeV	8 GeV
Circumference	259 m	269 m	562 m	845 m	1104 m	1436 m
Lattice type	DBA	DBA	DBA	DBA	DBA	DBA
Current	300 mA	400 mA	300 mA	200 mA	100 mA	100 mA
Hor. emittance	7.4 nm	4.4 nm	2.7 nm	4 nm	3.1 nm	3.4 nm





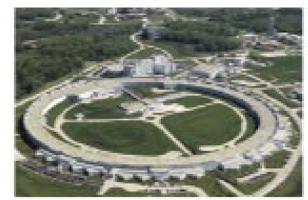
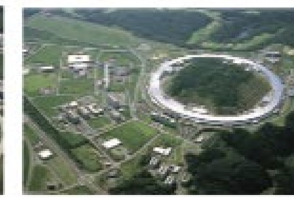

Ring parameters can be adjusted to meets specific requirements.
Presented parameters are typical operational parameters.

Choice of Beam Energy

Advantages of higher electron beam energy:

- Easier to produce high-energy photons (hard x-rays).
- Better beam lifetime.
- Easier to achieve higher current without encountering beam instabilities.

Disadvantages of higher beam energy:

- Higher energy beams have larger emittances (reduced brightness) for a given lattice.
- Stronger (more expensive) magnets are needed to steer and focus the beam.
- Larger rf system needed to replace synchrotron radiation energy losses.
- Many modern machines settle around 3 - 5 GeV

Typical Applications of Light Sources
Protein Crystallography

SPRING 8
Japan

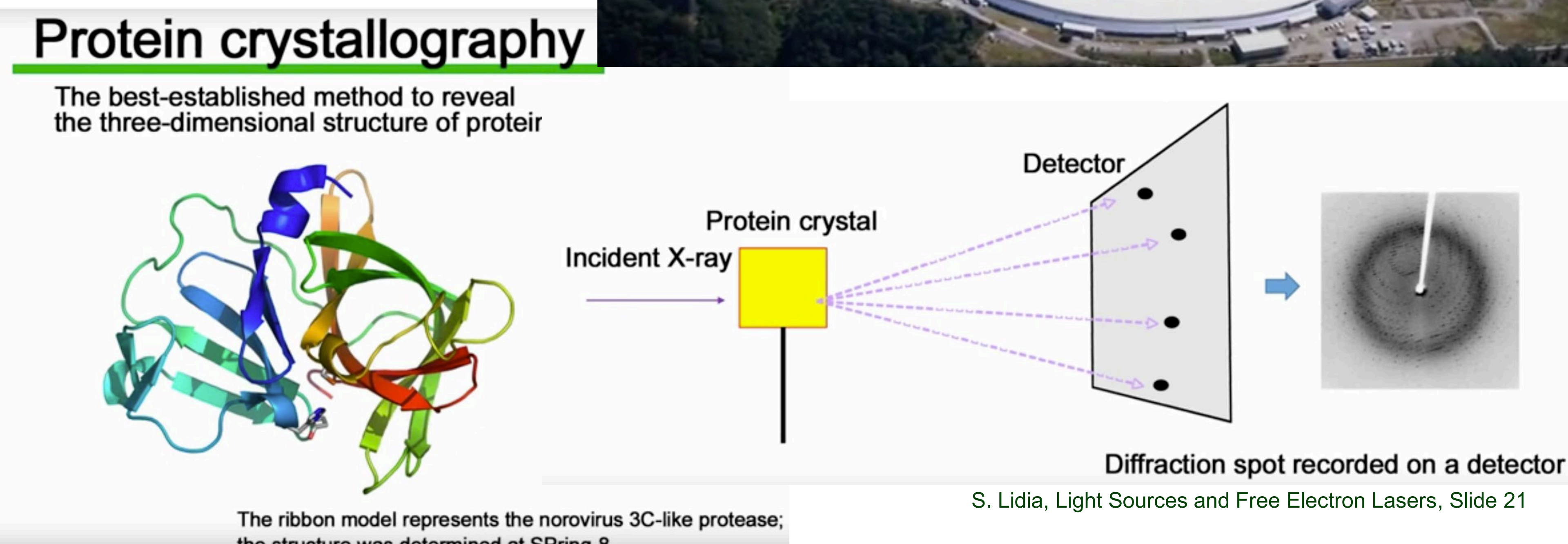

Preparation and Execution Of Experiments

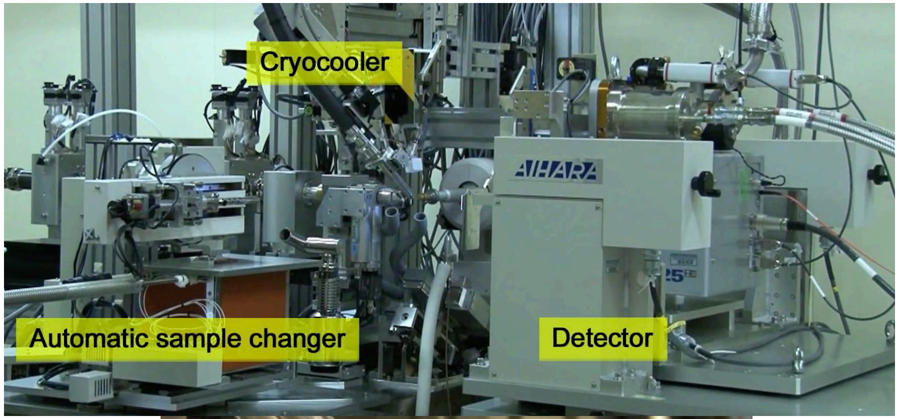

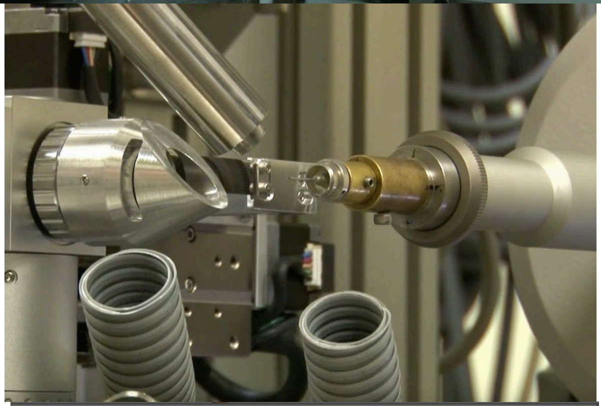

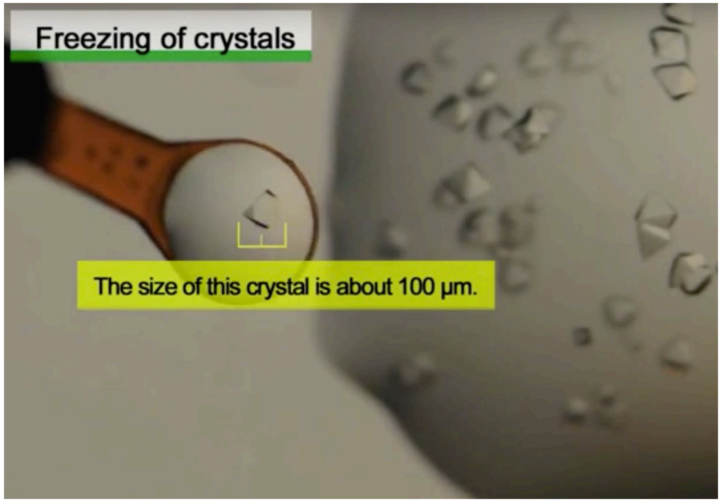

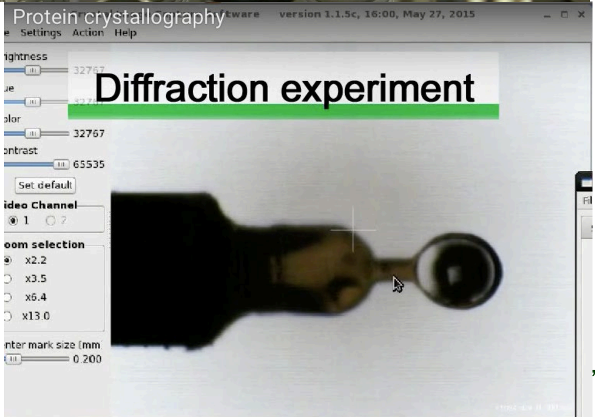

Result Processing

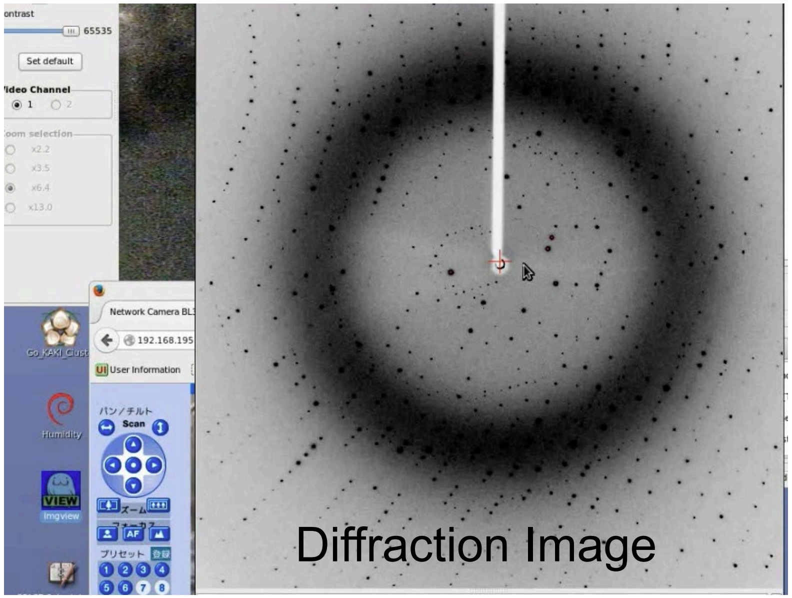
Diffraction Image

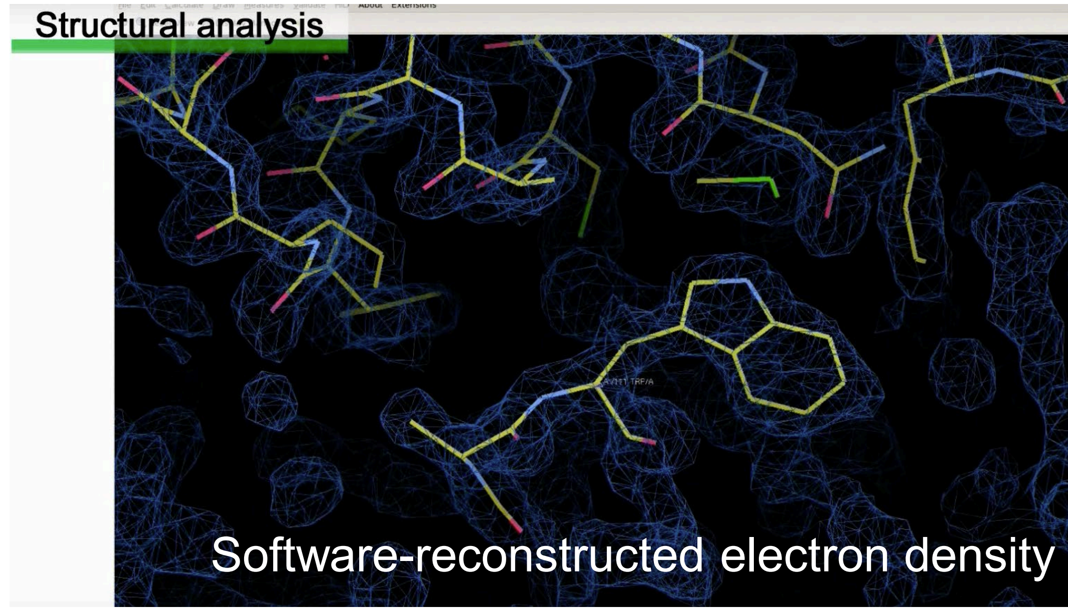
Structural analysis

Software-reconstructed electron density

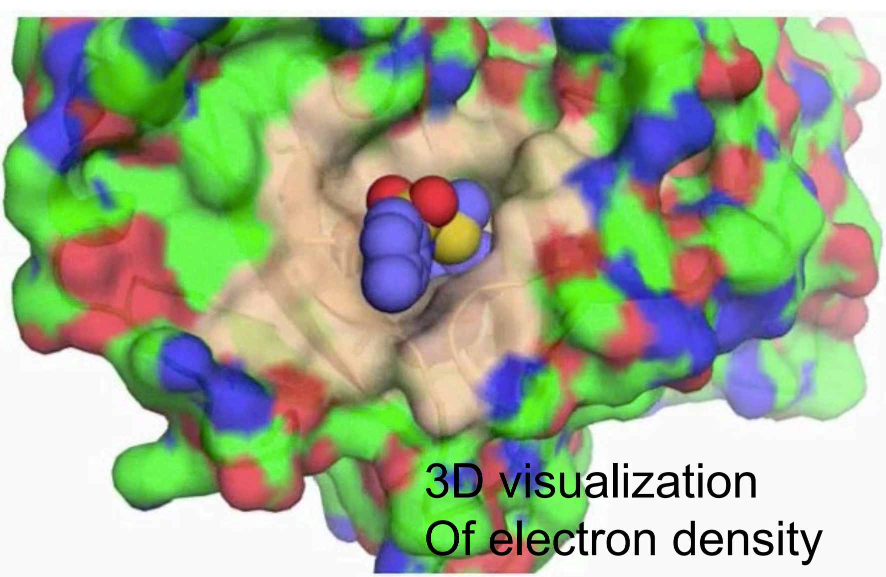
3D visualization
Of electron density

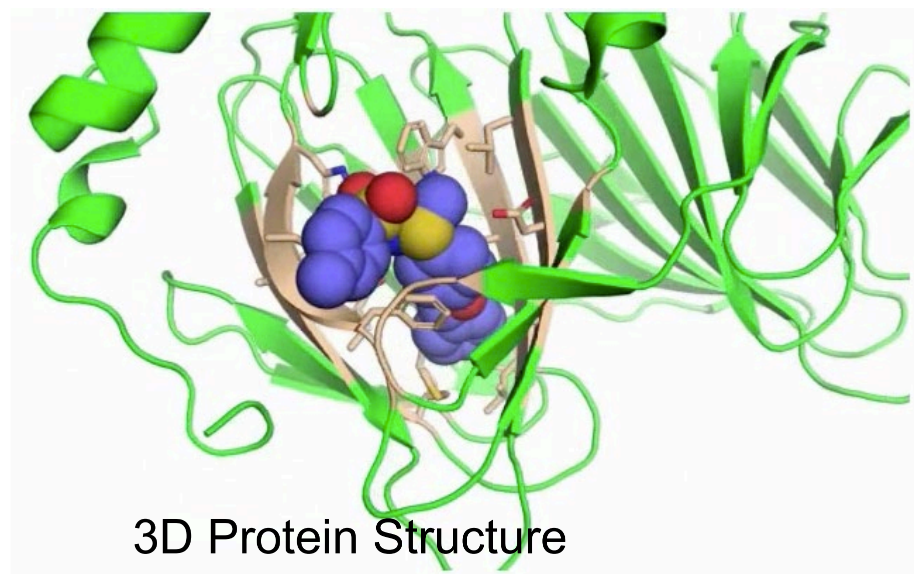
3D Protein Structure

Developing High Brightness Synchrotrons

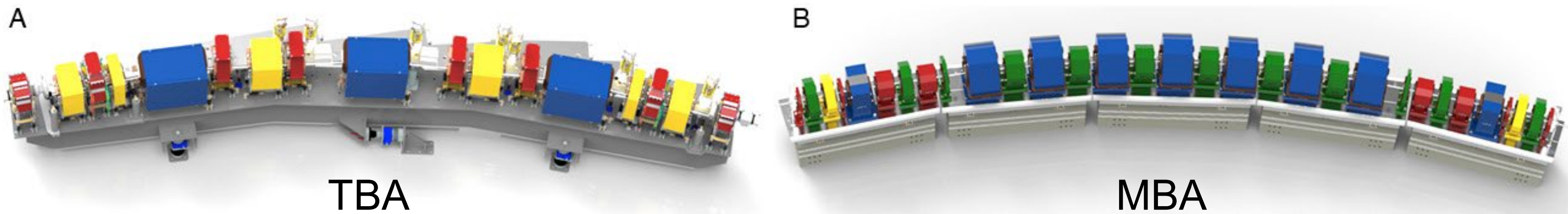

Development of Multi-Bend Achromat (MBA) lattices to replace 3rd Generation Triple Bend Achromats (TBA)

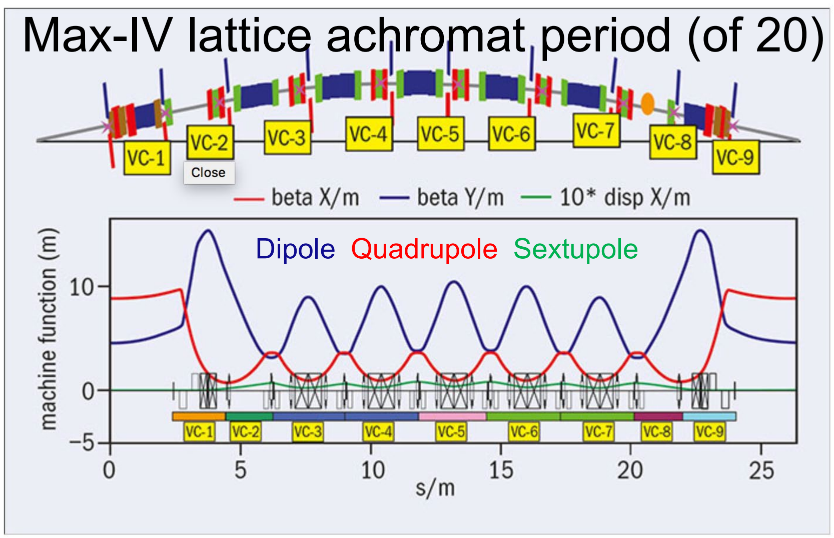

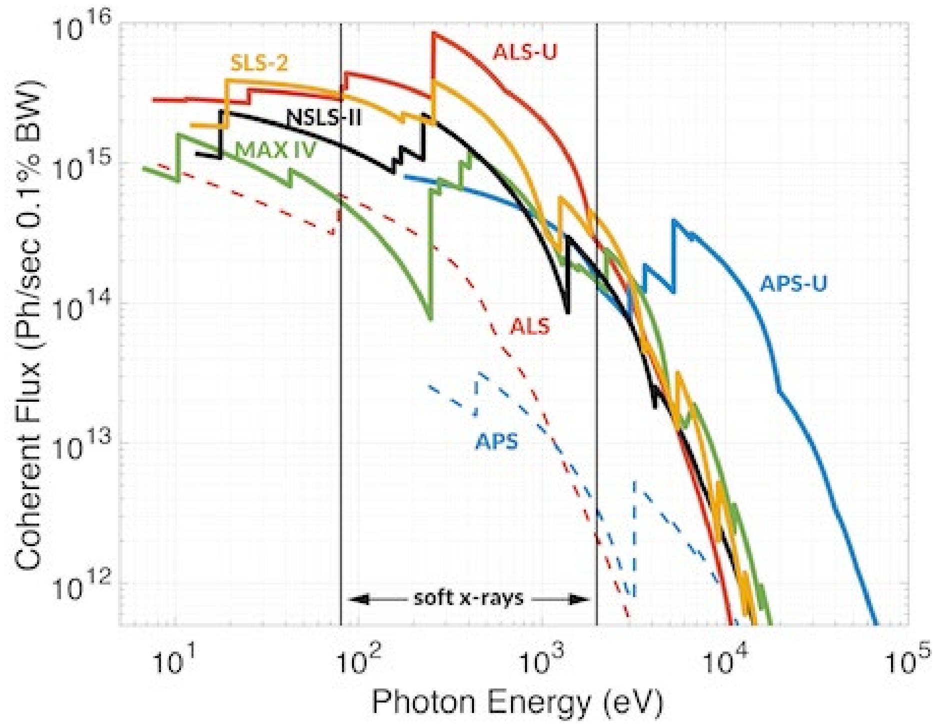

MBA Upgrade Increases Beam Brightness for Diffraction Limited X-rays

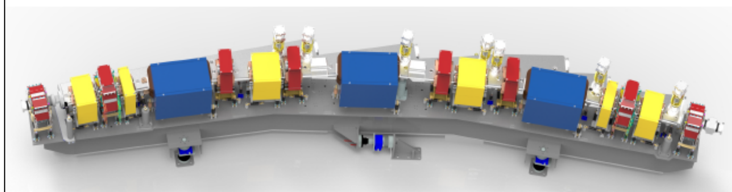

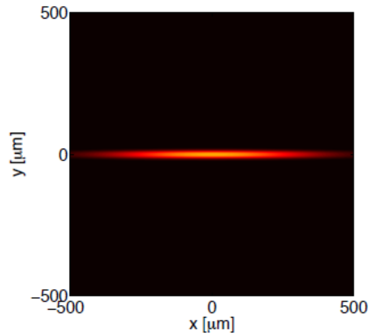

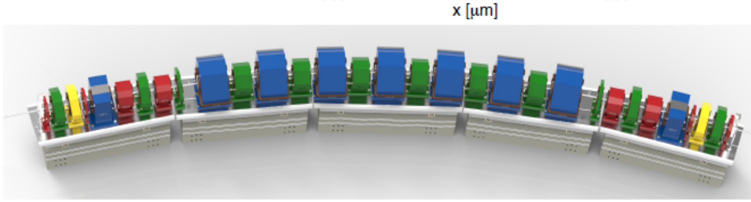

Nearly diffraction limited soft xrays

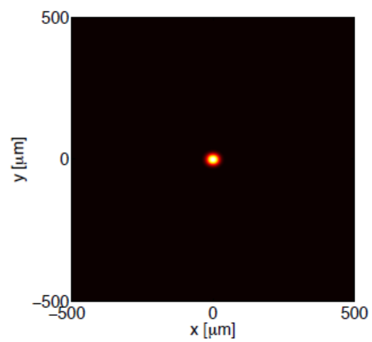

Parameter	Units	ALS	ALS-U
Electron energy	GeV	1.9	2.0
Horiz. emittance	pm	2000	~50
Vert. emittance	pm	30	~50
Beamsize @ ID center (σ_x/σ_y)	µm	251 / 9	<10 / <10
Beamsize @ bend (σ_x/σ_y)	µm	40 / 7	<5 / <7
bunch length (FWHM)	ps	60-70 (harmonic cavity)	120-200 (harmonic cavity)
RF frequency	MHz	500	500
Circumference	m	196.8	~196.5

BERKELEY LAB

ALS-U

Free Electron Lasers

- Free electron lasers operate on the principle of electromagnetic instability involving three components:
  - A relativistic electron beam
  - A magnetic undulator (K<1)
  - A co-propagating radiation (EM) field
- The undulator field couples with the transverse electron motion and allows a transverse current to interact with the transverse EM electric field.
- The EM field modulates the beam energy, producing bunching and debunching over the EM wavelength.

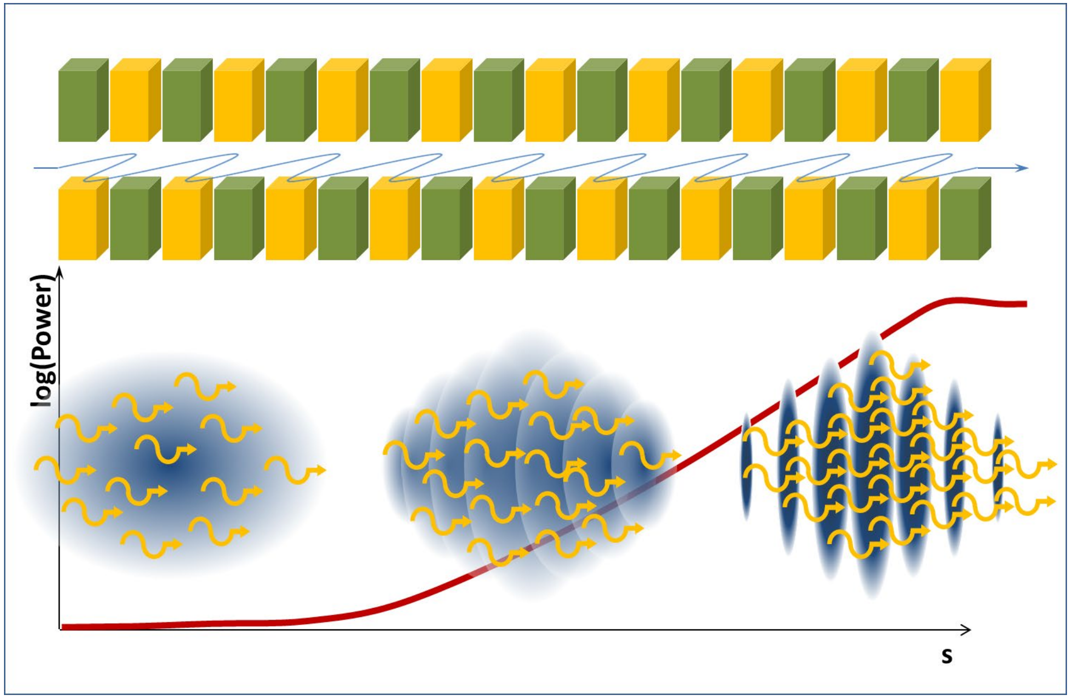

- Microbunching further enhances the coherent coupling between electron and photon field → <u>gain</u>
- These system can operate in oscillator or amplifier configurations
- Lack of available optics for hard x-rays means that only amplifier configurations are possible
  - Self-Amplified Spontanaeous Emission (SASE) and Cascaded High Gain Harmonic Generation (HGHG) processes

Storage Ring and Linac FELs

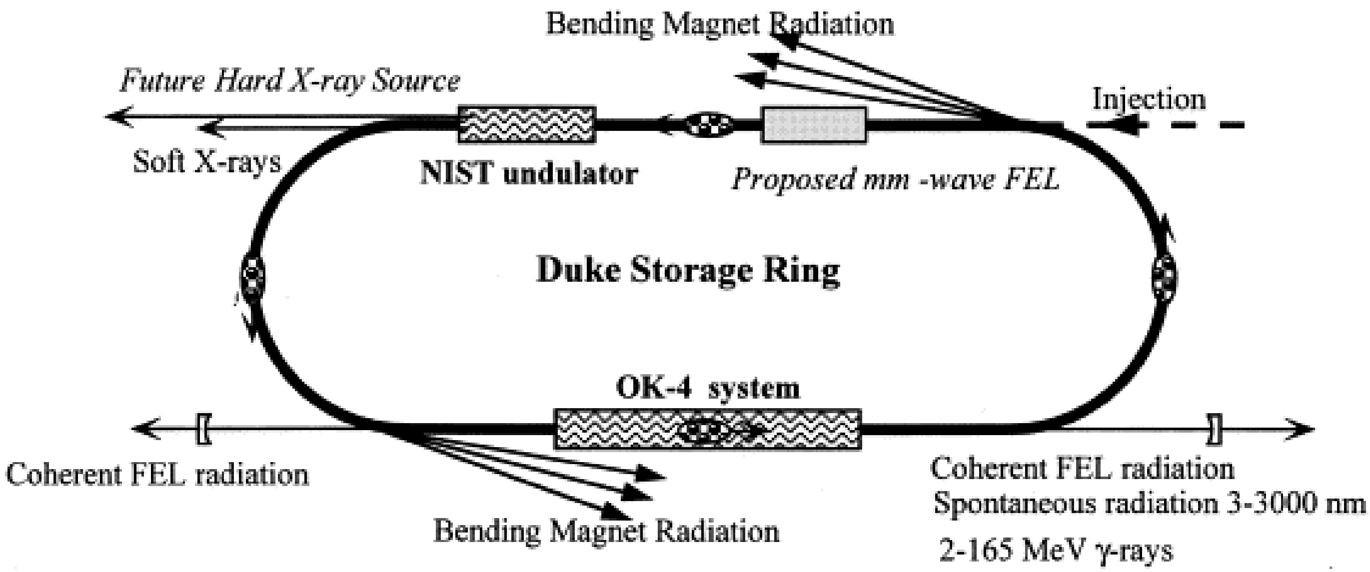

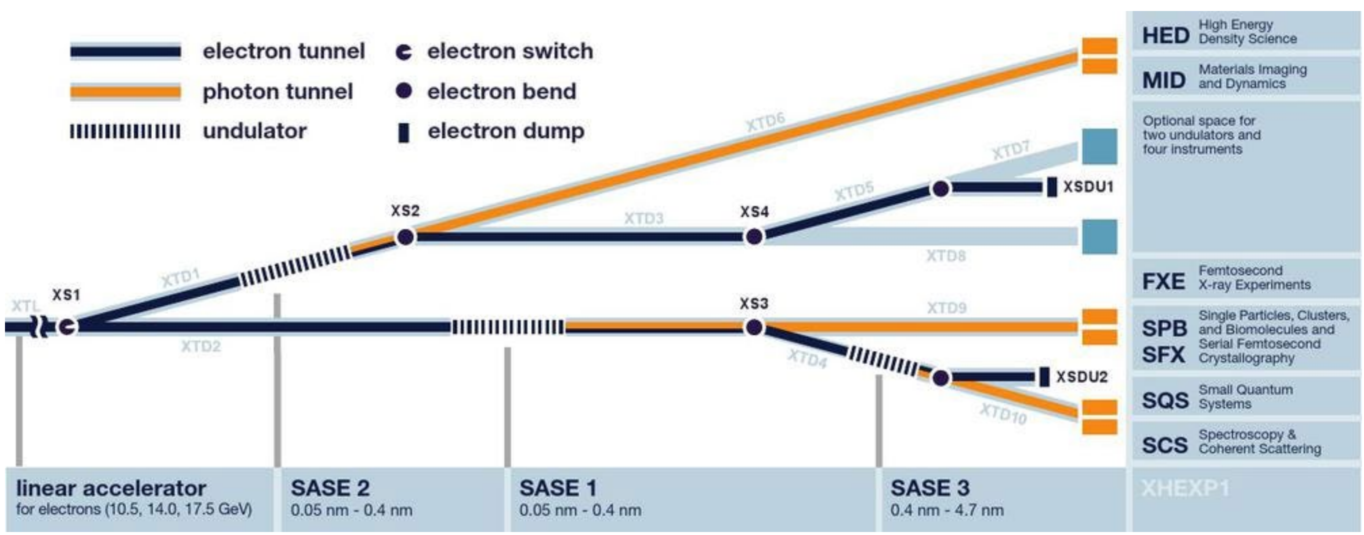

1-D Gain and Scaling in High Gain Regime

- Linear gain regime
  - Microbunches form and become well defined
  - Slippage carries photons to different microbunches
  - Radiated power is increasing exponentially
    $P_{rad}(z) = P_0 e^{z/L_{gain}}$ -- power amplifier
  - Microbunch energy spread increases
  - 'Cooperation' length (l_c) is the amount of slippage that occurs over a gain length
- Saturation
  - The field saturates after a length $L_{sat} \approx 20\ L_{gain}$
  - Radiated power is $P_{sat} = \rho_{FEL} I_{beam} E_{beam}$
- Caveats (ie. what are the hidden assumptions?)
  - Optimal phase space overlap between electron and photon beams
    - » $\varepsilon_\perp < \lambda/4\pi$
  - Relative energy spread should be smaller than FEL parameter $\sigma_\delta < \rho_{FEL}$

$$L_{gain} \approx \frac{\lambda_u}{4\sqrt{3}\rho_{FEL}}$$

$$\rho_{FEL} = \left[\frac{K}{4\gamma}[JJ]^2 \frac{\omega_p}{\omega_u}\right]^{2/3}$$

$$\omega_p^2 = 4\pi r_e c^2 n_e/\gamma$$

$$l_c \approx \frac{\lambda_{rad}}{\lambda_u} L_{gain}$$

Linac Coherent Light Source (LCLS)

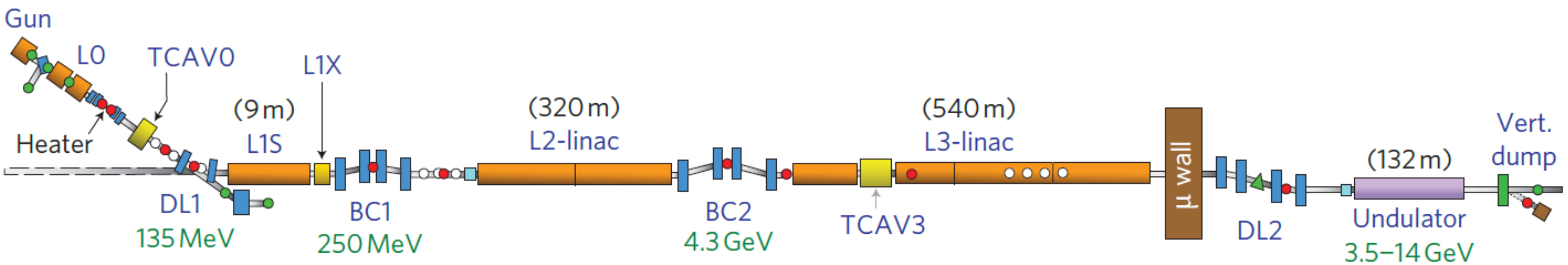

Table 1 | Design and typical measured parameters for both hard (8.3 keV) and soft (0.8–2.0 keV) X-rays. The 'design' and 'hard' values are shown only at 8.3 keV. Stability levels are measured over a few minutes.

Parameter	Design	Hard	Soft	Unit
Electrons				
Charge per bunch	1	0.25	0.25	nC
Single bunch repetition rate	120	30	30	Hz
Final linac e^- energy	13.6	13.6	3.5–6.7	GeV
Slice† emittance (injected)	1.2	0.4	0.4	μm
Final projected† emittance	1.5	0.5–1.2	0.5–1.6	μm
Final peak current	3.4	2.5–3.5	0.5–3.5	kA
Timing stability (r.m.s.)	120	50	50	fs
Peak current stability (r.m.s.)	12	8–12	5–10	%
X-rays				
FEL gain length	4.4	3.5	~1.5	m
Radiation wavelength	1.5	1.5	6–22	Å
Photons per pulse	2.0	1.0–2.3	10–20	10^{12}
Energy in X-ray pulse	1.5	1.5–3.0	1–2.5	mJ
Peak X-ray power	10	15–40	3–35	GW
Pulse length (FWHM)	200	70–100	70–500	fs
Bandwidth (FWHM)	0.1	0.2–0.5	0.2–1.0	%
Peak brightness (estimated)	8	20	0.3	10^{32} *
Wavelength stability (r.m.s.)	0.2	0.1	0.2	%
Power stability (r.m.s.)	20	5–12	3–10	%

*Brightness is photons per phase space volume, or photons s^{-1} mm^{-2} $mrad^{-2}$ per 0.1% spectral bandwidth.
†'Slice' refers to femtosecond-scale time slices and 'projected' to the full time-projected (that is, integrated) emittance of the bunch.

Lasing at 1.5 Angstroms

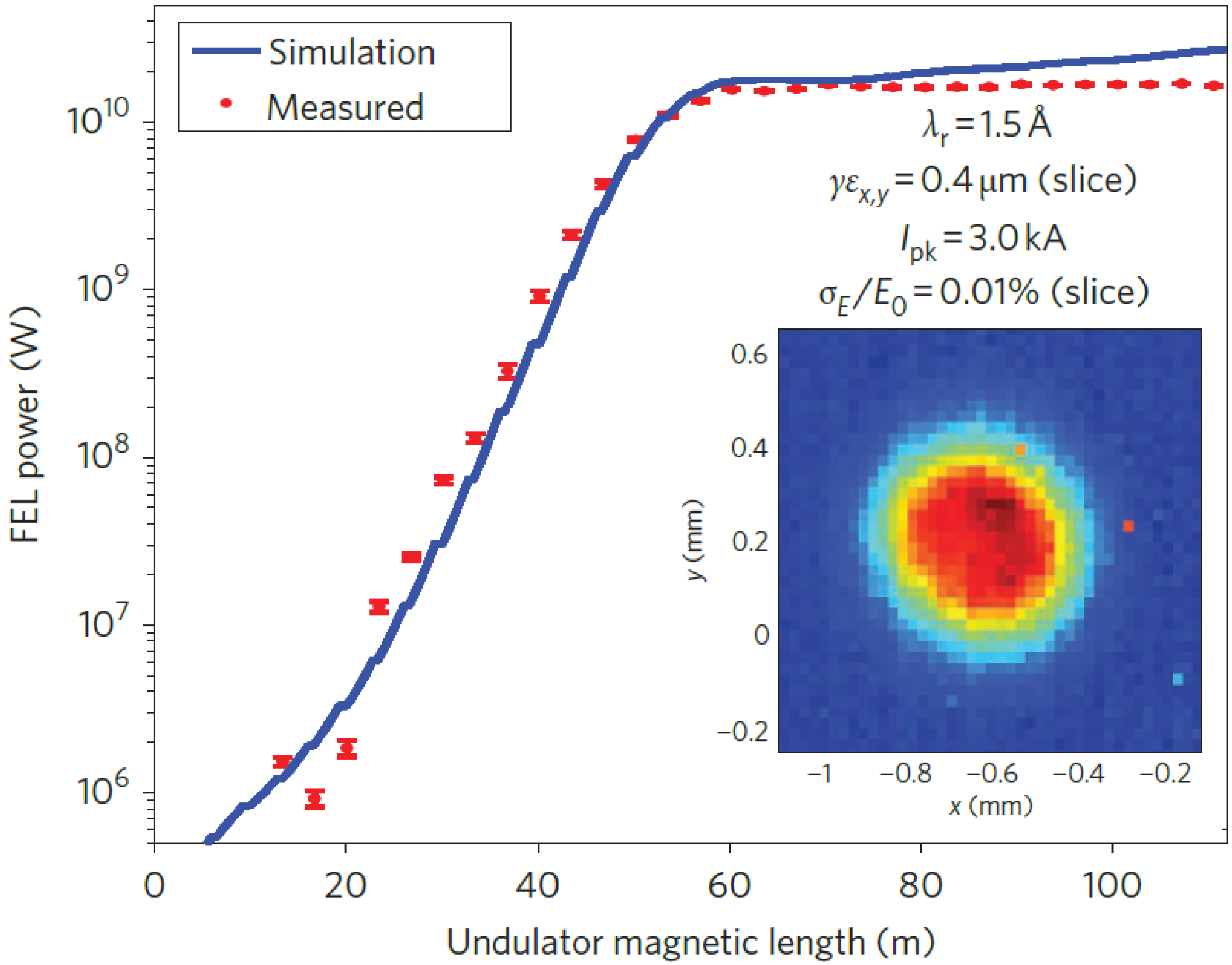

P. Emma, et al, Nature Photonics, v.4, Sept 2010.

Self Amplified Spontaneous Emission

- From 1-D gain

$$P_{rad}(z) = P_0 e^{z/L_{gain}}$$

- What happens when $P_0 = 0$?
- Startup from noise
  - Electron bunch is composed of distinct particles with randomized positions. Schottky noise exists over broad band.
  - Noise spectrum components at the fundamental wavelength (and harmonics) couple to the EM field
- Temporal coherence is lost

$$\frac{\Delta\omega}{\omega} \sim 2\rho \sim 10^{-3}$$

$$\left(\frac{\Delta\omega}{\omega}\right)_{spike} \sim \frac{1}{\sigma_T \omega} \sim 10^{-5}$$

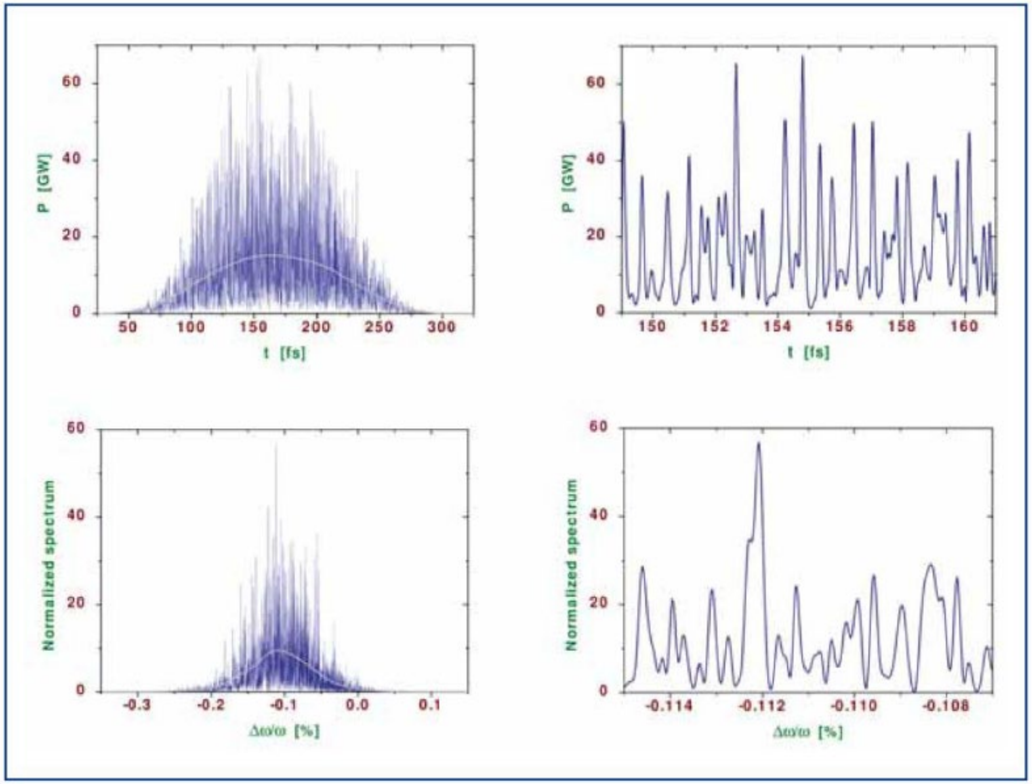

Figure 5.2.4 *Temporal (top) and spectral (bottom) structure for 12.4 keV XFEL radiation from SASE 1. Smooth lines indicate averaged profiles. Right side plots show enlarged view of the left plots. The magnetic undulator length is 130 m.*

Source: The European XFEL TDR – DESY 2006-097 (2006)

Two-Stage Cascaded Harmonic Generation

Seeded amplifiers can limit the growth of the noise spectrum

FERMI@elettra

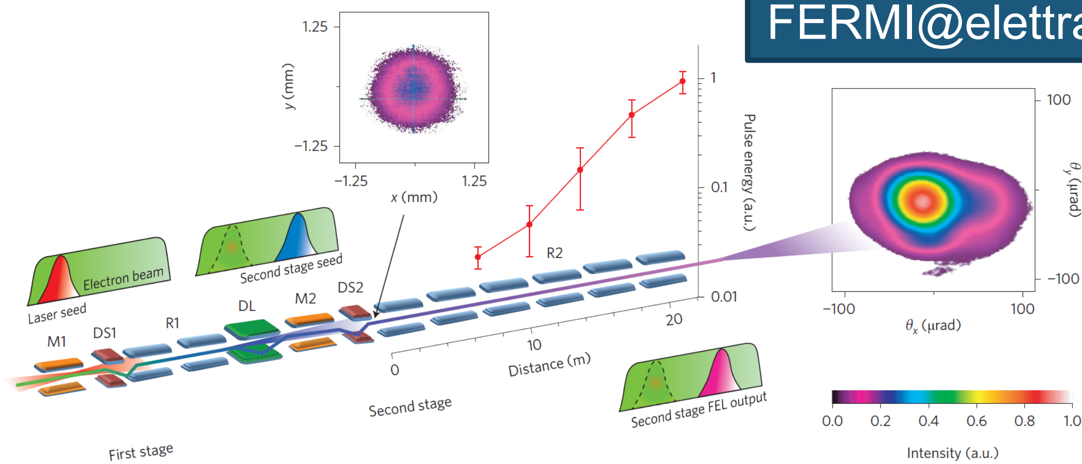

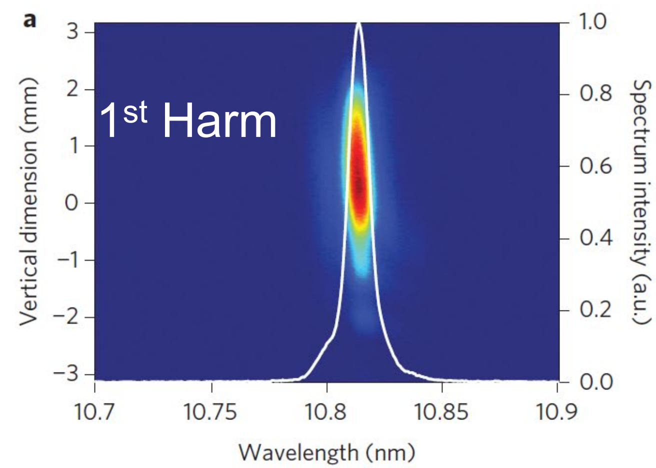

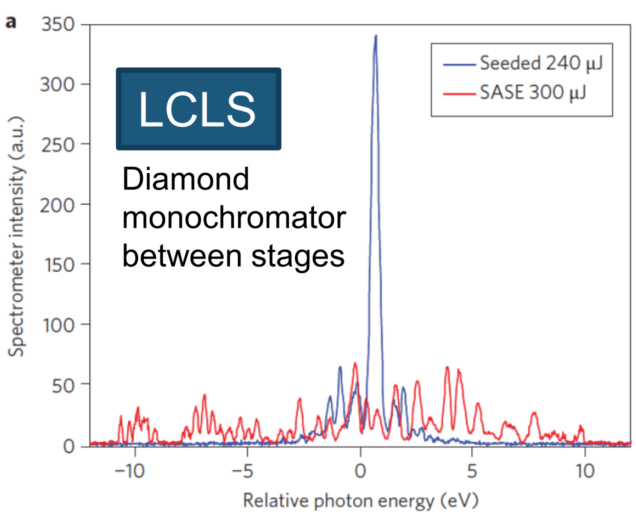

Stage 2 vs. Stage 1

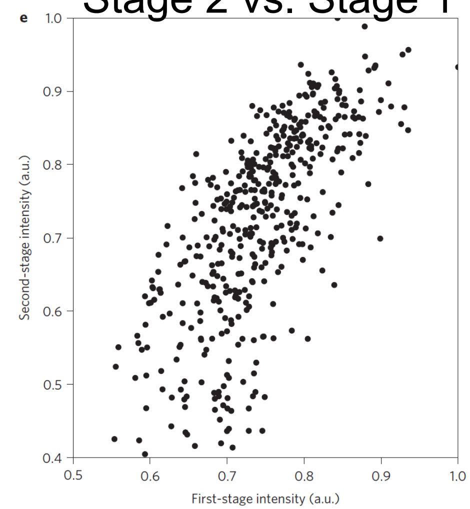

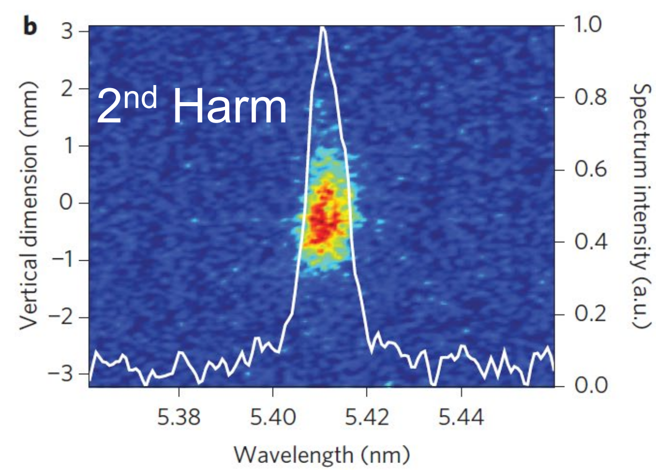

Amann, et al, Nature Photonics, v.6 October 2012

Allaria, et al, Nature Photonics, v.7, November 2013

Electron Beam Quality Determines Performance

- Electron beam injectors are pushing on brightness frontiers
  - Short bunches (< ps) and lower bunch charges (10s-100s pC)
- Emittance exchange methods (swap warm for cold phase spaces when needed)
- Increase incoherent energy spread to prevent longitudinal microbunching instabilities ('laser heater')

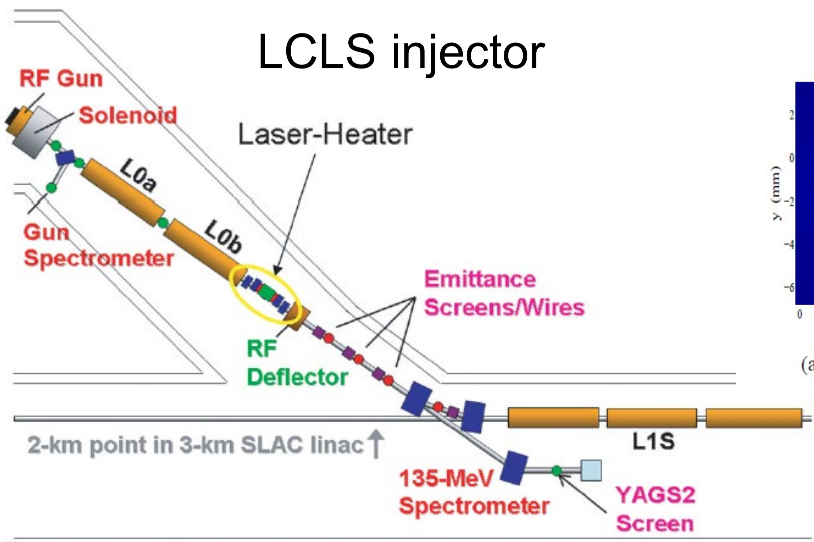

10 μJ 230 μJ

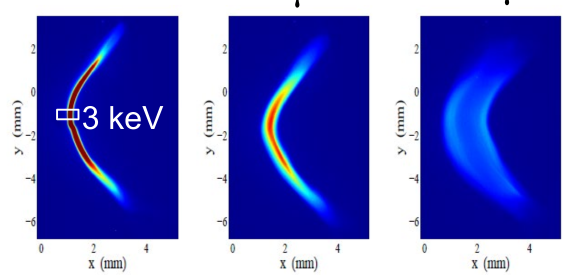

(a) no heating (b) nominal heating (c) maximum heating

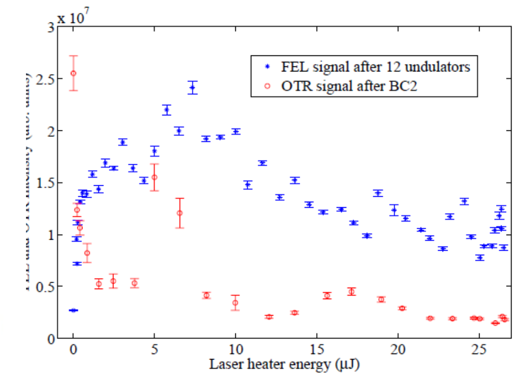

P. Emma, et al, SLAC-PUB-14338, 2009

Thank You!

Additional topics

- Undulator topics
  - Transverse multipoles
  - Phase errors
  - Variable polarization
- KMR equations
  - Simulation of bunching and beam intensity (1D)
  - SASE
  - Self-seeded hard xray
- 3D effects
  - Electron emittance – slice/projected, matching parameter
  - Optical diffraction, gain guiding
  - wakefields